

Towards Computationally Efficient Autocalibration for Accelerated MRI using Compressed Sensing Parallel Imaging

A. Brau¹, P. Lai¹, S. Narasimhan², B. Narayanan³, and V. Saradhi²

¹Global Applied Science Laboratory, GE Healthcare, Menlo Park, CA, United States, ²Computing & Decision Sciences Lab, GE Global Research, Bangalore, India,

³Medical Image Analysis Lab, GE Global Research, Bangalore, India

Introduction:

A number of highly accelerated data acquisition methods for 3D volumetric MRI using both Compressed Sensing and parallel imaging have been developed. Among them L1-SPIRiT[1], and an efficient version of it called ESPIRiT[2] have been proposed in the recent past. ESPIRiT addresses the computational challenges with the use of an image-domain Parallel imaging (PI) operator based on sensitivity maps obtained from a SPIRiT [4] convolution kernel, in place of performing computationally expensive convolution with the kernel in k-space in L1-SPIRiT. But the computation of the SPIRiT kernel weights itself is still computationally expensive, especially for high channel count reconstructions. The weights are computed by obtaining a least squares fit for predicting target points in the calibration region using a set of source points in their neighborhood. The computational complexity for generating the kernel weights is dependent on the number of source points and the number of target points. In the past, some approaches for optimal kernel support were explored in the context of GRAPPA [5]. This work is aimed at developing an optimally shaped neighborhood that reduces the number of source points without sacrificing image quality, but has much improved computational performance.

Theory:

The autocalibration procedure for ESPIRiT generates reconstruction weights \mathbf{w} by fitting a source matrix \mathbf{A} to a target matrix \mathbf{B} using generalized matrix inversion. Number of rows \mathbf{m} of \mathbf{A} , are the number of points in the calibration region. Conventional ESPIRiT calibration uses all source points in a cube-shaped k-space kernel. For a N -channel dataset with a kernel size of $k_1 k_2 k_3$, the number of columns \mathbf{n} are $k_1 k_2 k_3 N$. The weights for each coil are obtained by solving Moore-Penrose pseudo inverse [2] i.e., solve for $\mathbf{Cw}=\mathbf{D}$, where $\mathbf{C}=\mathbf{A}^T \mathbf{x} \mathbf{A}$, $\mathbf{D}=\mathbf{A}^T \mathbf{x} \mathbf{B}$. Coil-weights diminish rapidly, as k-space distance increases as shown in Figure 1(a). Based on this observation, the significance of source points formed by $k_1 \times k_2 \times k_3$ neighborhood around each target pixel was studied by experimenting with different neighborhoods defined by the L_p -neighborhood of the target point. If $\mathbf{X}_1=(x_1, y_1, z_1)$, $\mathbf{X}_2=(x_2, y_2, z_2)$ $\mathbf{E} \mathbf{R}^3$ the L_p distance $d_p(\mathbf{X}_1, \mathbf{X}_2)$ between \mathbf{X}_1 and \mathbf{X}_2 is defined as $(|x_1-x_2|^p + |y_1-y_2|^p + |z_1-z_2|^p)^{1/p}$. L_p -neighborhood of a point $\mathbf{X} \in \mathbf{E} \mathbf{R}^3$ for a kernel of radius r is defined as $\{\mathbf{Y} \in \mathbf{E} \mathbf{R}^3, \exists \mathbf{d}_p(\mathbf{X}, \mathbf{Y}) < r^p\}$. Different neighborhoods for $p=1, 2, \infty$ would take different shapes as shown in figure 1(a). For a typical kernel of radius $r=3$, an L_∞ kernel has 343 neighbors. The number of columns \mathbf{n} of matrix \mathbf{A} , goes down by a factor of 5.4 for an L_1 -neighborhood and by 2.78 for an L_2 -neighborhood. Since the solver is of the order of \mathbf{n}^3 , this gives an overall speed-up of 150x for an L_1 kernel and 21x for L_2 kernel over a typical box shaped L_∞ kernel. The correlation computation time for computing the correlation matrix \mathbf{C} scales down linearly.

Methods:

Based on the above theory, the calibration step mainly consists of the following operations: 1) Forming the \mathbf{A} matrix, based on the neighborhood shape. 2) Finding the correlation matrices $\mathbf{C}=\mathbf{A}^T \mathbf{x} \mathbf{A}$, $\mathbf{D}=\mathbf{A}^T \mathbf{x} \mathbf{B}$ 3) Solving for the kernel weights for each coil. Creating the matrix \mathbf{A} and finding the correlation matrix takes up significant memory and involves redundant computation. We exploit the redundancy and directly compute the correlation matrix as proposed in [3]. We experimented the method described above for L_p neighborhoods, with $p=0.1$ to 1 in steps of 0.1, for $p=2$ and $p=\infty$ on 4 patient datasets (T2-weighted brain MRI using 8-channels and 32 channels, Proton-density-weighted Knee MRI, noncontrast-enhanced renal MRA).

Results:

While we observed some difference in the image quality for $p < 1$, we found that for $p=1$, $p=2$, $p=\infty$ there was no visible difference in image quality. The ESPIRiT reconstruction outputs by using L_1, L_2, L_∞ norms for calibration weights computation are shown in figure 1(d). This is confirmed by the fit we observe between source and target points for these neighborhoods and the coil-maps generated as shown in figure 1(c). We implemented this approach on a dual Intel Xeon 55xx. With our multi-threaded implementation using 8-threads, for a 32-channel dataset, and a calibration region of size $27 \times 27 \times 128$, the compute time for the solver is 720 seconds for L_∞ kernel, 5 seconds for L_1 kernel, and 35 seconds for L_2 kernel.

Discussion:

Using an optimal neighborhood for calculating kernel weights for calibration in ESPIRiT, we can significantly improve the computational efficiency. This study demonstrates that we can achieve this, ensuring that we are not compromising on the fit between the source and target points from the calibration region and more importantly the perceptual image quality.

References:

[1] Lustig ISMRM, 2009:334; [2] Peng Lai ISMRM 2010:345 [3] P.J. Beatty, ISMRM 2007, 17:49 [4] Lustig M, MRM, 2010, 64:457 [5] Roger Nana, MRM, 2008, 59:819-825

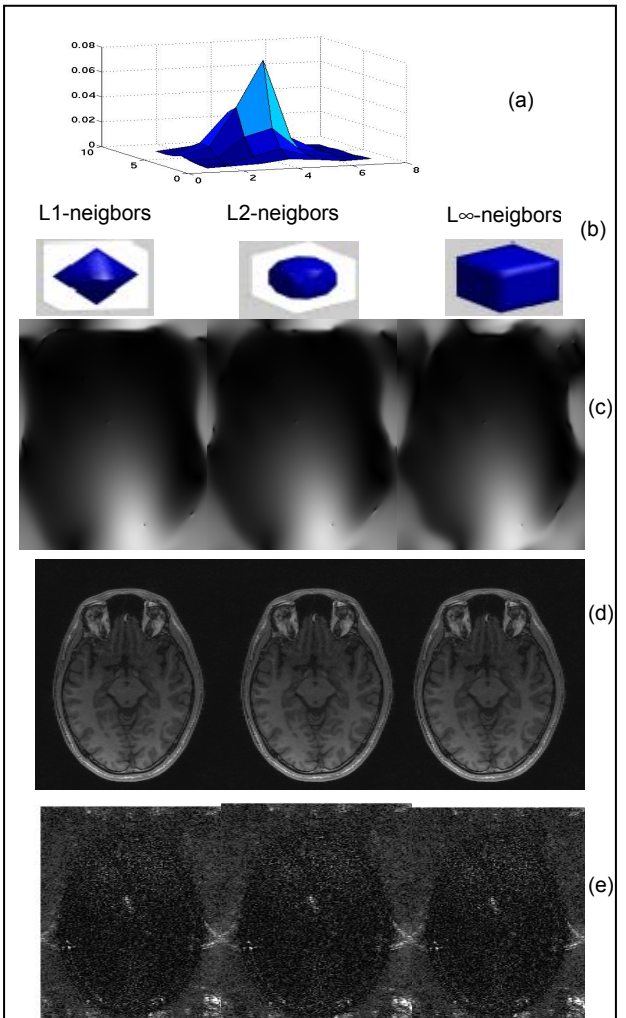


Figure 1: T2-weighted 32 channel Brain MRI (a) Plot of weights for a typical 7×7 neighborhood (b) Neighborhood shapes (c) Coil Maps (d) Final Output (e) difference Images with respect to fully sampled for L_1 , L_2 and L_∞ norms

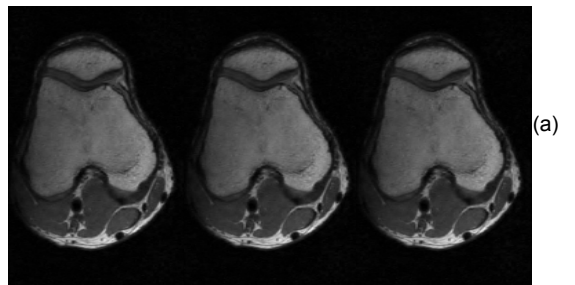


Figure 2: PDW- 8-channel Knee MRI: Final Output for L_1, L_2 and L_∞ norms